

Existence Conditions for Stable Stationary Solitons of the Cubic-Quintic Complex Ginzburg-Landau Equation with a Viscosity Term

Woo-Pyo Hong

Department of Electronics Engineering, Catholic University of Daegu, Hayang, Gyongsan,
Gyungbuk 712-702, South Korea

Reprint requests to W.-P. H.; E-mail: wphong@cu.ac.kr

Z. Naturforsch. **63a**, 757–762 (2008); received August 13, 2008

We report the existence of a new family of stable stationary solitons in the one-dimensional cubic-quintic complex Ginzburg-Landau equation with the viscosity term. By applying the paraxial ray approximation, we obtain the relation between the width and the peak amplitude of the stationary soliton in terms of the model parameters. We find the bistable solitons in the presence of the small viscosity term. We verify the analytical results by direct numerical simulations and show the stability of the stationary solitons. We conclude that the existence condition obtained by the paraxial method may serve as physically more reliable initial condition for stable stationary soliton propagation in the optical system modeled by the one-dimensional cubic-quintic complex Ginzburg-Landau equation with the viscosity term, of which analytical solution is not obtainable with all nonzero parameters.

Key words: One-Dimensional Cubic-Quintic Complex Ginzburg-Landau Equation; Viscosity Term;
Existence Conditions for Stationary Solitons; Numerical Simulation.

1. Introduction

The one-dimensional (1D) complex Ginzburg-Landau equation (CGLE) is one of the widely studied nonlinear equations for describing dissipative systems above the point of bifurcation [1]. The CGLE and its extension model a large variety of dissipative physical systems, such as binary fluid convection [2], electro-convection in nematic liquid crystals [3], patterns near electrodes in gas discharges [4], and oscillatory chemical reactions [5]. The continuous 1D CGLE possesses a rich variety of solutions including coherent structures such as pulses (solitary waves), fronts (shock waves), sinks (propagating hole with asymptotic negative group velocity), sources (propagating hole with asymptotic positive group velocity), periodic unbounded solutions, vacuum, periodic and quasi-periodic solutions, slowly varying fully nonlinear solutions, and a transition to chaos [6]. However, there are many models which contain some small additional terms for various applications. As such an interesting example, we consider the cubic-quintic complex Ginzburg-Landau equation (cqCGLE), which contains an additional viscosity term [7], in the form

$$\begin{aligned} i\psi_t + \frac{1}{2}\psi_{xx} + |\psi|^2\psi &= \alpha|\psi|^4\psi + iv\psi_{xx} \\ &\quad + i\varepsilon(|\psi|^2 - \beta|\psi|^4 - 1)\psi, \end{aligned} \quad (1)$$

where in the context of a nonlinear optical fiber system t denotes the propagation distance and x is the retarded time, ψ is the slowly varying envelope of the electric field in dimensionless form. The term with ε accounts for linear and nonlinear amplification, α is a higher-order correction term to the nonlinear refractive index, β is the dissipative term, and v describes spectral filtering [7–9]. In general, the viscosity term $iv\psi_{xx}$ is neglected, if the spectral filtering is not considered. Sakaguchi [7] has investigated the motions of pulses and vortices in the context of 1D and 2D versions of (1) without the viscosity term. The author has shown that there exist moving pulses and vortices with any velocities, because the equation is invariant for the Galilei transformation, in case of the zero viscosity term [7].

In fact, similar to (1) but more popular cqCGLEs have been introduced and many aspects of their properties have been investigated by both analytical and numerical methods [10, 11]. Fauve and Thual [10] have shown the existence of a bright solitary wave in the vicinity of the subcritical Hopf bifurcation of the cqCGLE. Soto-Crespo et al. [11] have found some exact soliton solutions and their stability has been investigated numerically. The regions for the existence of stable pulse-like solutions have been also identified. Later, Soto-Crespo et al. [12] have numerically found more interesting coherent structures such as pulsating,

erupting, and creeping solitons of the cqCGLE and their existences have been experimentally verified [13].

The purpose of the present work is to present the existence of a new family of stationary or nontraveling solitons of (1) in the presence of the viscosity term by adopting the paraxial ray approximation method [14, 15], which has been used to find stationary solitons in photorefractive materials [16, 17]. In particular, Hong [18] has recently found the conditions for the existence of stable stationary bright solitons in the context of the 1D CGLE with additional nonlinear gradient terms. By applying the paraxial method, we investigate the existence of stationary solitons of (1), even in the presence of the viscosity term, and reveal some of their interesting properties. Finally, we perform numerical simulations to show that the solitons are dynamically stable during their propagations which supports the paraxial ray approximation. As the analytic form of a sech-type solitary-wave solution can not be analytically obtained from (1), we compare the solution with the numerical evolution of a sech-type initial profile as initial condition.

2. Results

According to the paraxial theory of Akhmanov et al. [14], an optical beam or pattern preserves its structural form while propagating through the medium, i.e., the solution shows self-similar behaviour. This simple method can be applied to some nonintegrable equations to find initial profiles which preserve the self-similar behaviour [16, 17]. However, since the theory is not exact, its predictions need to be verified by detailed numerical simulations. In the following analysis, we look for a solution in the form

$$\psi = \Phi(x, t) \exp[-i\Omega(x, t)]. \quad (2)$$

We substitute this into (1) and obtain

$$\begin{aligned} \Omega_t \Phi + \frac{1}{2} \Phi_{xx} - \frac{1}{2} \Phi \Omega_x^2 + \Phi^3 - \alpha \Phi^5 \\ - v(2\Phi_z \Omega_z + \Phi \Omega_{xx}) = 0, \end{aligned} \quad (3)$$

$$\begin{aligned} \Phi_t - \Phi_x \Omega_x - \frac{1}{2} \Phi \Omega_{xx} - v(\Phi_{xx} - \Phi \Omega_x^2) \\ + \varepsilon(1 - \Phi^2 + \beta \Phi^4)\Phi = 0. \end{aligned} \quad (4)$$

We further assume that the lowest-order localized bright soliton, for which the envelope is confined in the central region of the soliton, i.e., $\Phi(x=0, t)_{\max} = Q$,

$\Phi(x, t) = 0$ as $|x| \rightarrow \infty$, and the wave solution, maintains its self-similar character while it propagates [16, 17]. Hence, the ansatz solution of the above equation can be written as

$$\begin{aligned} \Phi(x, t) &= \sqrt{\frac{P}{f(t)}} \exp\left[-\frac{x^2}{2r^2 f^2(t)}\right], \\ \Omega(x, t) &= \frac{x^2}{2} \frac{d \ln f(t)}{dt}, \end{aligned} \quad (5)$$

where P is the peak amplitude at $x = 0$ and $f(t)$ is the variable pulse width parameter so that $rf(t)$ is the width of the soliton. We show in the following that the pulse radius r can be found as functions of the system parameters. Substituting (5) into (3) and (4), using the paraxial approximation [15–17], Taylor expanding it with respect to x , and equating the coefficients of x^2 of (3) and (4), respectively, we obtain

$$\begin{aligned} \frac{d^2 f(t)}{dt^2} - \frac{10\alpha P^2}{r^2 f(t)^3} + \frac{6P}{r^2 f(t)^2} \\ - \frac{1}{2} \frac{(\frac{d}{dt} f(t))^2}{f(t)} - \frac{3}{r^4 f(t)^3} = 0, \\ 2v f(t)^2 \frac{df(t)}{dt} r^4 + 5f(t) \frac{df(t)}{dt} r^2 \\ + [-4\varepsilon f(t)^2 + 12\varepsilon Pf(t) - 20\varepsilon P^2 \beta] r^2 - 12v = 0. \end{aligned} \quad (6)$$

Since we are interested in a nonsingular bright soliton at $t = 0$, we first look for the equilibrium point of the ordinary differential equation, which can be obtained by setting $f(t) = 1$ and $df(t)/dt = 0$. Thus, in the following analysis, we denote r as the width of the soliton. We then obtain two equations, which give the relation among the width r , the system parameters, and the peak amplitude P , as

$$r^2 = \frac{3}{2P(3f - 5\alpha P)}, \quad (7)$$

$$r^2 = \frac{3v}{\varepsilon(3Pf - f^2 - 5\beta P^2)} \quad (8)$$

from (3) and (4), respectively. Two possible amplitudes P in terms of the system parameters from the consistency requirement of the above two equations can be obtained as

$$\begin{aligned} P_{\pm} = \{ -3\varepsilon + 6v \pm \\ [(-20\beta + 9)\varepsilon^2 + (40\alpha - 36)v\varepsilon + 36v^2]^{1/2} \} \\ \cdot \{ 10(-\beta\varepsilon + 2v\alpha) \}^{-1}. \end{aligned} \quad (9)$$

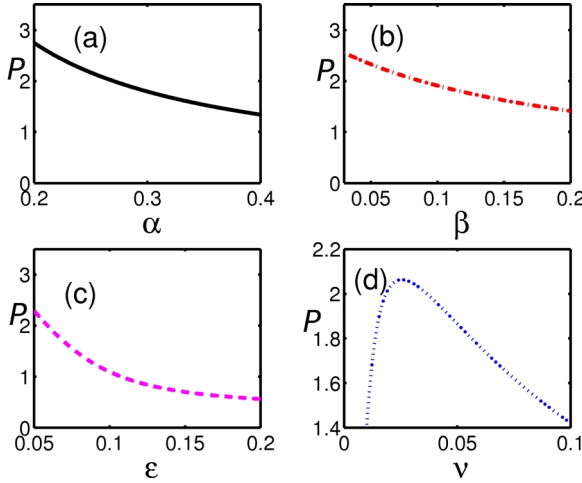


Fig. 1. Variation of width square r^2 versus system parameters. For all figures, α varies in $0.2 \leq \alpha \leq 0.4$. (a) P decreases with increasing α at fixed $\beta = 0.10$, $\varepsilon = 0.02$, and $v = 0.05$. (b) P decreases with increasing β for $0.03 \leq \beta \leq 0.2$ at fixed $\varepsilon = 0.02$ and $v = 0.05$. (c) P rapidly decreases with increasing ε for $0.05 \leq \varepsilon \leq 0.2$ at fixed $\beta = 0.10$ and $v = 0.05$. (d) Two sets of value v corresponding to the same P exist with increasing v for $0.01 \leq v \leq 0.10$ at fixed $\beta = 0.10$ and $\varepsilon = 0.02$.

Finally, we obtain four possible solutions for the bright solitons (r^2, P_{\pm}) according to (7)–(9). Depending on the parameters of the system under consideration, one may choose a physically allowed solution, i. e., $P > 0$ and $r^2 > 0$. It is interesting to note that the width and amplitude are functions of the system parameters without having any constraint among them, in contrast to many single hump bright-type solitary wave solutions found in extended 1D CGLEs [19]. In the following, we consider the case for $P = P_+$ so that the width is finally expressed as

$$r^2 = \frac{3}{2P_+(3f - 5\alpha P_+)}. \quad (10)$$

Before proceeding further, we would like to find analytical solutions of (1) in the sech-type.

Figure 1 shows the relations between the peak amplitude with respect to the variations of the system parameters. In fact, since the parameter space for $\alpha, \beta, \varepsilon, v$ is huge, which depends on the system under consideration, we select some arbitrary parameters for illustration purposes, however, maintaining their values much smaller than 1.0. We choose α as a common variation parameter of Figs. 1a–d in the range of $0.20 \leq \alpha \leq 0.40$ since it is present in the denominator of (10). Figure 1a shows an anti-correlation between

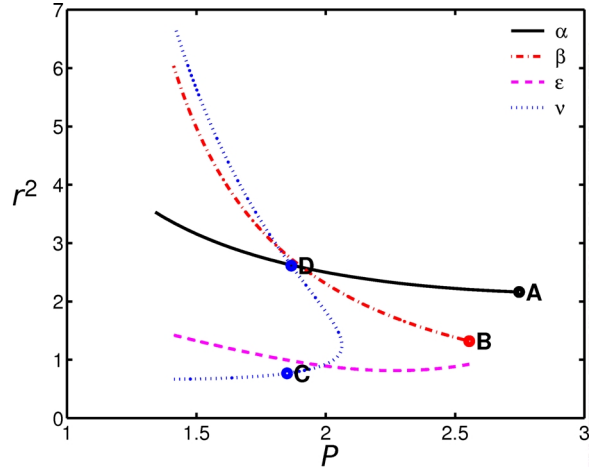


Fig. 2. Variation of width square r^2 versus peak amplitude P corresponding to the system parameter variations in Figs. 1a–d, respectively. Any points, for example A, B, C, and D, on these curves represent stationary solitons. The width of soliton decreases with increasing P . The points C and D are bistable solitons because of two sets of width for the same P due to the presence of the small viscosity term v .

P and α for increasing α at fixed $\beta = 0.10$, $\varepsilon = 0.02$, and $v = 0.05$. As depicted in Fig. 1b, P also decreases with increasing β for $0.03 \leq \beta \leq 0.2$ at fixed $\varepsilon = 0.02$, and $v = 0.05$. Figure 1c shows a more rapid decrease in P with increasing ε in the range of $0.05 \leq \varepsilon \leq 0.2$ at fixed $\beta = 0.10$ and $v = 0.05$. Finally, an interesting feature in Fig. 1d is that two sets of v value corresponding to the same P exist with increasing v in the range $0.01 \leq v \leq 0.10$ at fixed $\beta = 0.10$ and $\varepsilon = 0.02$.

As seen in Fig. 2, each point (r^2, P) on the curves corresponding to the change of parameters as shown in Figs. 1a–d, respectively, represents the existence condition found in (10) for stationary solitons. For the cases of the existence curves corresponding to the parameter changes in Figs. 1a–c, respectively, all widths of the solitons decrease with increasing P . On the other hand, as shown in Fig. 2d, there appear two sets of width for the same P , i. e., two sets of bright soliton pairs denoted by the points C and D, even in the presence of a small v value in the range of $0.01 \leq v \leq 0.05$. It is interesting to note that this bistable feature resembles to the existence condition for stable stationary solitons in photorefractive media [15–17], however, it is different in the sense that two sets of soliton pairs exist with the same spatial width but having two different peak powers.

To verify the predictions of the analytical results, which are based on the paraxial approximation

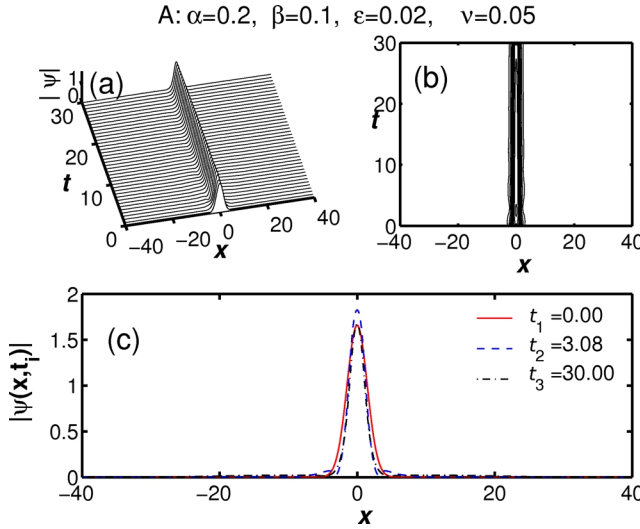


Fig. 3. (a) Numerically simulated propagation of a stationary soliton with the width square $r_A^2 = 2.16$ and the peak amplitude $P_A = 2.74$. The stable propagation confirms the analytical result obtained by the paraxial ray approximation. (b) Contour plot of (a). (c) Snapshots of profile at different times. The initial pulse adjusts itself at $t = 3.08$ by having a brief breathing behaviour, after which it remains a stable stationary entity.

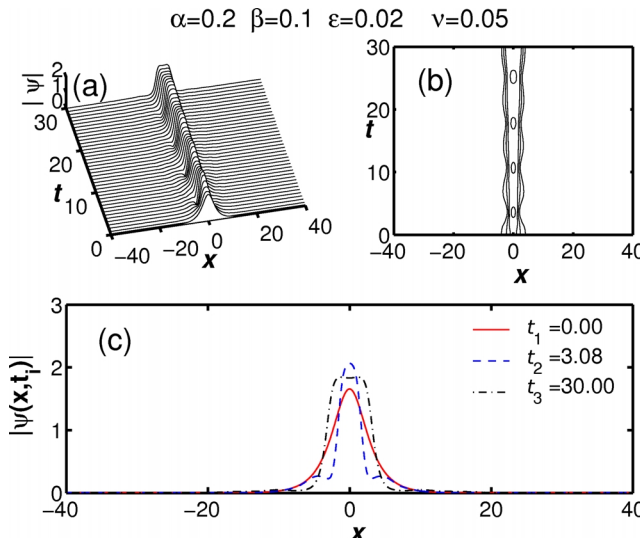
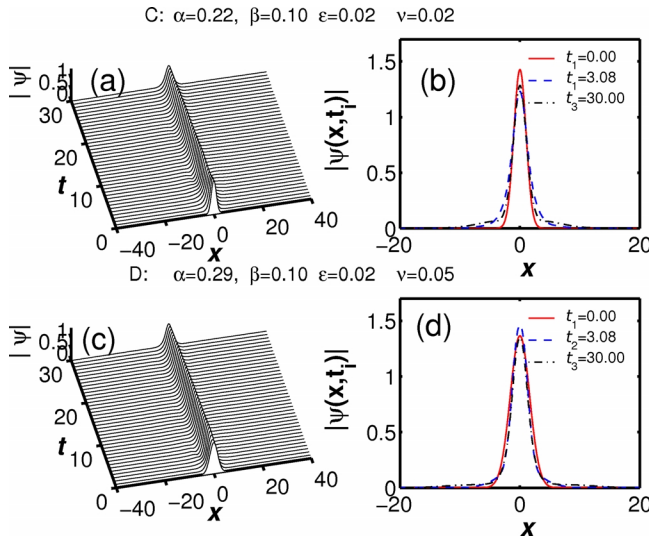
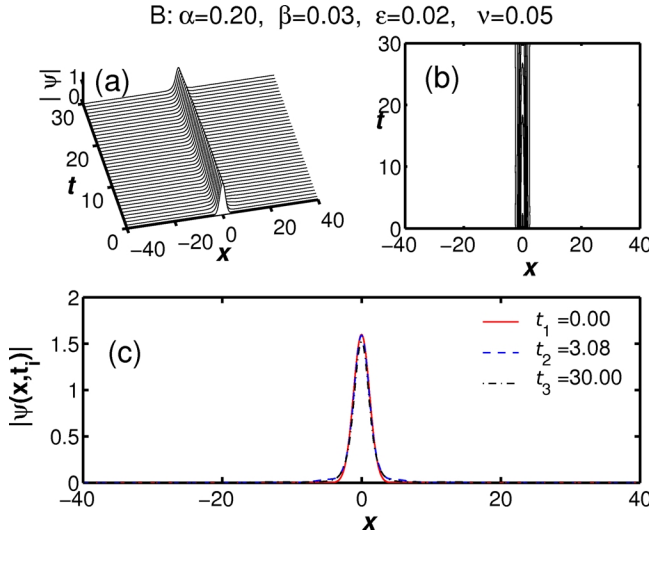


Fig. 4. (a) Propagation of the initial sech profile in the form of $\psi(x, 0) = \sqrt{P_A} \operatorname{sech}(x/r_A^2)$ by using the same system parameters as A in Figure 3. (b) Contour plot of periodic pulsations. (c) Snapshot at $t = 3.08$ shows oscillatory tails on the left- and right-hand sides of the wave. The initial profile transforms into a front at $t = 30.0$.

[14, 15], we perform a numerical simulation of (1) for the soliton solutions randomly chosen parameters denoted by A, B, C, and D in Fig. 2, by adopting the widely used split-step Fourier method and taking the Crank-Nicholson implicit scheme for time propagation under periodic boundary conditions [20, 21] with the initial profile provided by the width and peak amplitude. The numerical simulations are carried out by varying the number of discrete Fourier modes between $N = 1024$ and $N = 4096$, and various time steps between 10^{-2} and 10^{-3} .

The results of the direct numerical simulation for the case of solution parameters denoted by A in Fig. 2, i.e., $\alpha = 0.20$, $\beta = 0.1$, $\varepsilon = 0.02$, $v = 0.05$, $r_A^2 = 2.16$,

and $P_A = 2.74$, are presented in Figure 3. As shown in Figs. 3a and b for the modulus of amplitude $|\psi|$ and for its contour plot, respectively, the initial profile provided in the form of $\psi = \sqrt{P} \exp(-x^2/2r^2)$ maintains good stability during its propagation. According to the snapshots in Fig. 3c, the initial pulse adjusts itself at $t = 3.08$ by showing brief breathing behaviour, after which it remains as a stable stationary entity, confirming the stability of the soliton. As the result of such adjustment, the width of the soliton at $t = 30$ (dot-dashed line) slightly decreases, however, its peak amplitude remains the same as the initial profile (solid line). Next, we would like to compare the propagation of the solution obtained by the paraxial approximation with an



initial sech profile in the form of $\psi = \sqrt{P} \operatorname{sech}(x/r^2)$, since there is no exact sech-type solution found for (1) without the constraint among the parameters (see some of the sech-type solutions obtained in [19]). By using the same system parameters as for A, we plot the simulated results in Figure 4. It is evident from Figs. 4a and b that the initial sech profile goes through periodic pulsations before turning into a front. Unlike the brief width adjustment in Fig. 3c, the snapshot at $t = 3.08$ in Fig. 4c shows oscillatory tails on the left- and right-hand sides of the wave, which are attributed to the larger width of the sech pulse in comparison with that of the solution in Figure 3.

Fig. 5. (a) Simulated propagation of a stationary soliton with the width square $r_B^2 = 1.32$ and the peak amplitude $P_B = 2.56$. In comparison with Fig. 3, the invariance of the initial profile is more clearly demonstrated when β decreases from $\beta = 0.1$ to $\beta = 0.03$. (b) Contour plot of (a). (c) Snapshots of profile at different times. The soliton profile at $t = 3.08$ shows a brief width adjustment before returning to the same initial peak amplitude at $t = 30.0$.

Fig. 6. Propagations of the bistable stationary solitons. (a) and (b) Propagation of the solution and its snapshots with $r_C^2 = 1.03$ and $P_C = 1.87$, respectively. Broadenings on both the left- and right-hand sides appear. (c) and (d) Propagation of the solution and its snapshot with $r_D^2 = 2.61$ and $P_D = 1.87$, respectively. More stable soliton propagation is observed after short width adjustment at $t = 3.08$.

Figure 5 shows the propagation of the initial profile with $r_B^2 = 1.32$ and $P_B = 2.56$ from the parameters $\alpha = 0.20$, $\beta = 0.03$, $\varepsilon = 0.02$, and $v = 0.05$ of B. According to the evolution and contour plots in Figs. 5a and b, respectively, and in comparison with the evolution of the soliton solution of the parameter A in Fig. 3, the invariance of the initial profile is more clearly demonstrated when β decreases from $\beta = 0.1$ to $\beta = 0.03$. As seen in the snapshots of Fig. 5c, the soliton profile at $t = 3.08$ again shows a brief width adjustment before returning to the peak amplitude of the initial profile, confirming the robustness of the soliton.

We now investigate propagations of the bistable stationary solitons with the parameters C and D marked on the existence curve in Fig. 2, of which the widths and peak amplitudes are given as $r_C^2 = 1.03$ and $r_D^2 = 2.61$ with $P_C = P_D = 1.87$, respectively. We note that even though both α and v increase from $\alpha = 0.22$ and $v = 0.02$ in C to $\alpha = 0.29$ and $v = 0.05$ in D, respectively, the stability of both solitons is maintained. However, as depicted in Figs. 6a and b, for the case of a narrow width r_C^2 , the propagated soliton widths at $t = 3.08$ and $t = 30.0$, respectively, show broadenings on both the left- and right-hand sides. On the other hand, for the case of larger width r_D^2 , more stable soliton propagation is observed in Fig. 6c after short width adjustment at $t = 3.08$, as depicted in Figure 6d. Even though not presented here, we have numerically confirmed that for other bistable solution parameters along the existence curve similar stability is maintained.

3. Conclusion

By adopting the paraxial ray approximation method used for seeking spatial solitons in a photorefractive medium [16, 17], we have found four existence conditions for the stationary solitons of the 1D cqCGLE with the viscosity term in (1). The parameter space of the peak amplitude and pulse width for such station-

ary bright solitons have been identified. In particular, it has been found that the peak amplitude is a function of the system parameters without having any constraint among them. Even in the presence of a small viscosity term, as shown in Fig. 2, we have found that there exist bistable solitons. The results of numerical simulations have been presented in Figs. 3–6 by selecting some of the solutions on the existence curves in Figure 2. We have observed that propagations of stable stationary bright solitons can be achieved when the initial wave profile is provided by the stationary soliton solution. We would like to stress that the paraxial approximation does not give the condition for absolutely robust soliton propagations, in the sense that, when the solution used as an initial wave, the profile has gone through a brief width adjustment transition before turning into a stable soliton. However, we have understood that the existence condition obtained by the paraxial method may serve as a physically more reliable initial condition for stable stationary soliton propagation in the optical system with the viscosity term modeled by (1), of which an analytical sech-type solution is not obtainable.

Acknowledgements

This work was supported by Catholic University of Daegu, South Korea in 2008.

- [1] I. S. Aranson and L. Kramer, Rev. Mod. Phys. **74**, 99 (2002).
- [2] P. Kolodner, Phys. Rev. A **44**, 6448 (1991).
- [3] M. Dennin, G. Ahlers, and D. S. Cannell, Phys. Rev. Lett. **77**, 2475 (1996).
- [4] K. G. Müller, Phys. Rev. A **37**, 4836 (1988).
- [5] Y. Kuramoto, Chemical Oscillations, Waves and Turbulence, Springer, Berlin 1984.
- [6] E. Yomba and T. C. Kofané, Chaos, Solitons and Fractals **15**, 197 (2003).
- [7] H. Sakaguchi, Physica D **210**, 138 (2005).
- [8] G. P. Agrawal, Phys. Rev. A **44**, 7493 (1991).
- [9] Y. S. Kivshar and G. P. Agrawal, Optical Solitons, Academic Press, London 2003.
- [10] S. Fauve and O. Thual, Phys. Rev. Lett. **64**, 2821 (1990).
- [11] J. M. Soto-Crespo, N. N. Akhmediev, V. V. Afanasjev, and S. Wabnitz, Phys. Rev. E **55**, 4783 (1997).
- [12] J. M. Soto-Crespo, N. Akhmediev, and A. Ankiewicz, Phys. Rev. Lett. **85**, 2937 (2000).
- [13] S. T. Cundiff, J. M. Soto-Crespo, and N. Akhmediev, Phys. Rev. Lett. **88**, 073903 (2002).
- [14] S. A. Akhmanov, A. P. Sukhorukov, and R. V. Khokhlov, Sov. Phys. USP **10**, 609 (1968); S. A. Akhmanov, A. P. Sukhorukov, and R. V. Khokhlov, in: Laser Handbook, Vol. II (Eds. A. T. Arechi, E. D. Shulz Dubois), North Holland, Amsterdam 1972, p. 1151.
- [15] S. Konar and A. Sengupta, J. Opt. Soc. Am. B **11**, 1644 (1994).
- [16] S. Jana and S. Konar, Phys. Lett. A **362**, 435 (2007).
- [17] S. Jana and S. Konar, Opt. Commun. **273**, 324 (2007).
- [18] W. Hong, Z. Naturforsch. **62a**, 368 (2007).
- [19] K. Maruno, A. Ankiewicz, and N. Akhmediev, Physica D **176**, 44 (2003); A. Ankiewicz, K. Maruno, and N. Akhmediev, Phys. Lett. A **308**, 397 (2003).
- [20] J. A. C. Heideman and B. M. Herbst, SIAM J. Num. Ann. **23**, 485 (1986).
- [21] W. P. Hong, Z. Naturforsch. **60a**, 719 (2005); **61a**, 23 (2006).